



Mushtaq, M., Wani, M. I., Saquib, S., [Ahmad, M.](#), Somappa, L., Baghini, M. S., [Heidari, H.](#) and Malik, S. (2023) Mismatch and Offset-Voltage Compensation Technique for Current Excitation Based Resistive Sensors Interface. In: 21st IEEE Interregional NEWCAS Conference (IEEE NEWCAS 2023), Edinburgh, UK, 26-28 June 2023, ISBN 9798350300246 (doi: [10.1109/NEWCAS57931.2023.10198102](https://doi.org/10.1109/NEWCAS57931.2023.10198102))

There may be differences between this version and the published version.
You are advised to consult the published version if you wish to cite from it.

<https://eprints.gla.ac.uk/297091/>

Deposited on 24 April 2023

Enlighten – Research publications by members of the University of Glasgow
<http://eprints.gla.ac.uk>

Mismatch and Offset-Voltage Compensation Technique for Current Excitation Based Resistive Sensors Interface

Mehreeq Mushtaq

*Centre of Sensors, Instrumentation and
Cyber Physical System Engineering
Indian Institute of Technology Delhi
National Institute of Technology Srinagar
mehreeqmushtaq@gmail.com*

Mohammad Idris Wani

*Centre of Sensors, Instrumentation and
Cyber Physical System Engineering
Indian Institute of Technology Delhi
New Delhi, India
idz228152@iitd.ac.in*

Sadan Saquib

*Centre of Sensors, Instrumentation and
Cyber Physical System Engineering
Indian Institute of Technology Delhi
New Delhi, India
idz228154@iitd.ac.in*

Meraj Ahmad

*School of Engineering
University of Glasgow
Glasgow, UK
Meraj.Ahmad@glasgow.ac.uk*

Laxmeesha Somappa

*Department of Electrical Engineering
Indian Institute of Technology Bombay
Mumbai, India
laxmeesha@ee.iitb.ac.in*

Maryam Shojaei Baghini

*Department of Electrical Engineering
Indian Institute of Technology Bombay
Mumbai, India
mshojaei@ee.iitb.ac.in*

Hadi Heidari

*School of Engineering
University of Glasgow
Glasgow, UK
Hadi.Heidari@glasgow.ac.uk*

Shahid Malik

*Centre of Sensors, Instrumentation and
Cyber Physical System Engineering
Indian Institute of Technology Delhi
New Delhi, India
smalik@iitd.ac.in*

Abstract—Resistive sensors have been increasingly used in a number of wearable biomedical applications ranging from prosthetic control to electronic skin, thanks to their miniaturized size. However, most resistive sensor systems suffer thermoelectric offset, large baseline resistance, and drift in baseline resistance. In addition, the system should be battery-operated and consume low power. In this paper, we present a pulse current excitation-based half-bridge mixed-signal interface circuit for accurate and high-resolution resistance measurement of resistive sensors. The circuit utilizes synchronous demodulation and a DC-Servo loop to compensate for the offset and mismatch to enhance the accuracy and measurement range. The circuit provides a linear output voltage proportional to the incremental change in sensor resistance. A prototype of the proposed system is developed and tested. The circuit compensates offset-voltage as high as ± 1.4 Volts and the resistance mismatch up to $100\text{ k}\Omega$ for a supply voltage of 3.3 Volts with an error of less than $\pm 1\%$.

Index Terms—Resistive sensors, interface circuit, high-sensitivity, high-resolution, auto-zeroing, synchronous demodulation.

I. INTRODUCTION

The applications of sensors in the biomedical area are increasing day by day with the advancement in different sensing materials and nanotechnology. Resistive sensors occupy a significant share of the wearable biomedical market. Resistive sensors have simple geometry and can be integrated with the current CMOS technology [1], [2]. Thanks to these features, they have been widely used to measure force and pressure for

prosthetic applications [3], surgical instruments [4], electronic skin [5], [6], [7] and so on. However, the performance of resistive sensors is affected by several factors, such as the thermoelectric offset voltage, large baseline resistance, drift in the baseline resistance, and parasitic capacitance. These non-idealities affect the performance of resistive sensors and limit their applications [8], [9]. In addition, the baseline resistance difference (BRD) will vary from sensor to sensor and, therefore, needs to be compensated for each sensor.

Wheatstone bridge-based signal conditioning circuits are widely used for resistive sensors [10]. The Wheatstone bridge compensates for the effect of the baseline resistance of the sensor. However, the output voltage of the conventional Wheatstone bridge-based circuit is non-linear with respect to the change in resistance for the signal element resistive sensors [11]. The non-linearity affects the sensitivity of the system with a wide dynamic range [12]. The Wheatstone bridge-based circuits are modified by including an auto-nulling feedback loop [13], [14], [15]. However, the auto-nulling loop, implemented using an analog multiplier for phase-sensitive-detection (PSD), increases the supply voltage requirement and power consumption of the overall sensor system, which is undesirable for the miniaturized battery-operated wearable sensor systems [16]–[18]. Digital potentiometers are nowadays utilized in the Wheatstone bridge for canceling the BRD [4]. However, due to finite resolution and large tolerance,

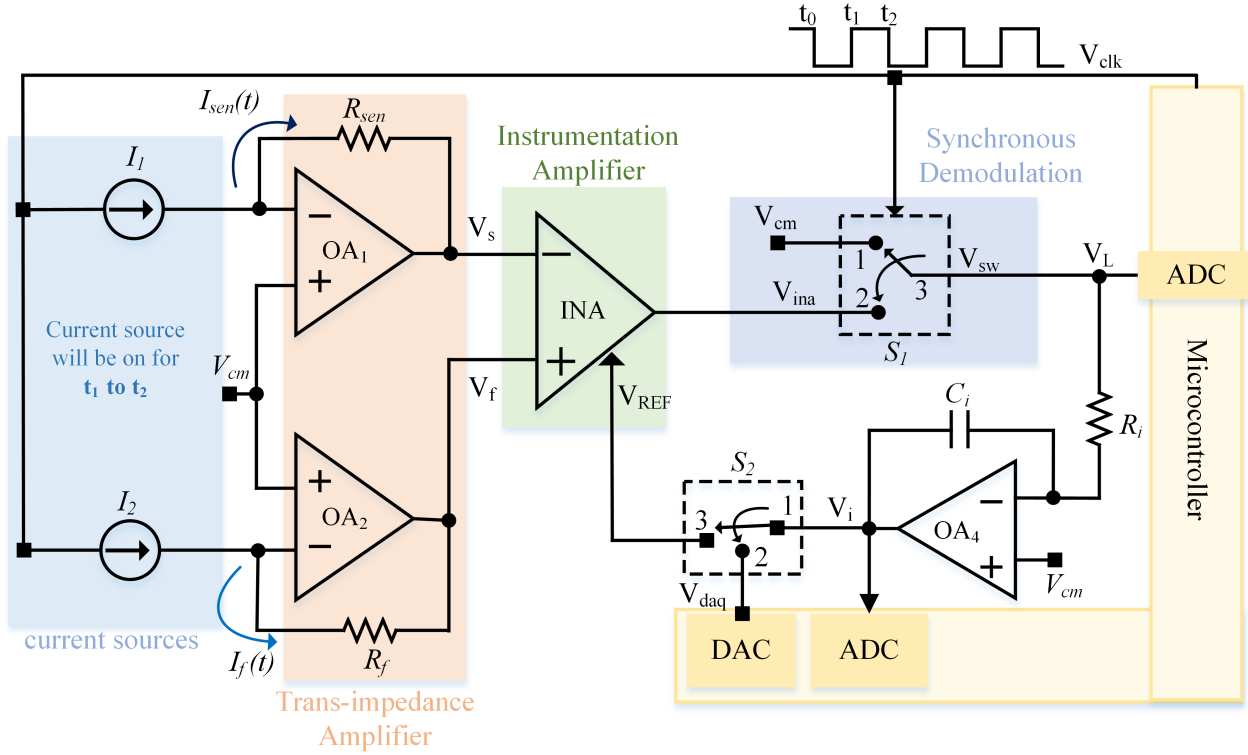


Fig. 1. Block diagram of the pulse current excitation-based proposed interface circuit for resistive sensors.

they are not effective. Moreover, for different sensors, the baseline resistors will be different and may vary by large range. Therefore, we need to have an auto-compensation scheme to compensate for the BRD in the sensors.

In this paper, we present a mixed-signal resistive sensor interface circuit for biomedical applications. The circuit consists of a bidirectional current source and a half-bridge circuit. The proposed circuit is an improvement of the current excitation-based circuit reported earlier [19]–[23]. The features of the proposed circuit are as follows.

- **Baseline-Resistance and Offset-Voltage Calibration:** The proposed circuit provides a simple topology to compensate for the BDR and offset voltage. In addition, owing to the pulse excitation signal, offset voltage can be monitored, and the resultant variation and drift can be compensated.
- **Low-Voltage Low-Power Interface:** Thanks to a pulse excitation signal, the proposed circuit operates on low voltage (3.3 V) and consumes low-power (around 3 mW) for off-the-shelf implementation of analog blocks.

II. PROPOSED SENSOR INTERFACE

The proposed interface circuit for resistive sensors is shown in Fig. 1. The circuit consists of two pulse current sources controlled by a square-wave clock pulse V_{clk} . The sensor resistance (R_{sen}) is connected to the feedback of the operational amplifier (OA_1). The current I_{sen} flows through the sensor resistance. The trans-impedance amplifier converts the

current into an equivalent voltage proportional to the sensor resistance. The trans-impedance amplifier configuration is used to establish enough voltage headroom across the current source to operate [23]. The voltage V_s can be written as follows.

$$V_s = \frac{V_{DD}}{2} - I_{sen}(t)R_{sen} \quad ; t_1 < \omega t < t_2 \quad (1)$$

The sensor resistance can be represented as a combination of baseline resistance R_o and change in the resistance (ΔR) due to the measurand. To compensate for the effect of baseline resistance, another branch with current I_f and resistance R_f , is added. The voltage at the output of the operational amplifier OA_2 can be written as follows.

$$V_f = \frac{V_{DD}}{2} - I_f(t)R_f \quad ; t_1 < \omega t < t_2 \quad (2)$$

An instrumentation amplifier (INA) is used to subtract the two signals. The output voltage of the instrumentation amplifier can be given as follows.

$$V_{ina} = I_{sen}(t)R_{sen} - I_f(t)R_f + V_{REF} \quad ; t_1 < \omega t < t_2 \quad (3)$$

Generally, the reference resistor R_{REF} is kept equal to the baseline resistance (R_o) of the sensor either manually or using a digital-potentiometer. However, due to finite resolution, the BRD is not compensated completely. This affects the accuracy of the system. To remove this, we used a switch-based demodulation and DC servo-loop. The output voltage V_{ina} is applied at one of the terminals of a single-pole-double-throw (SPDT) switch with other input of the switch

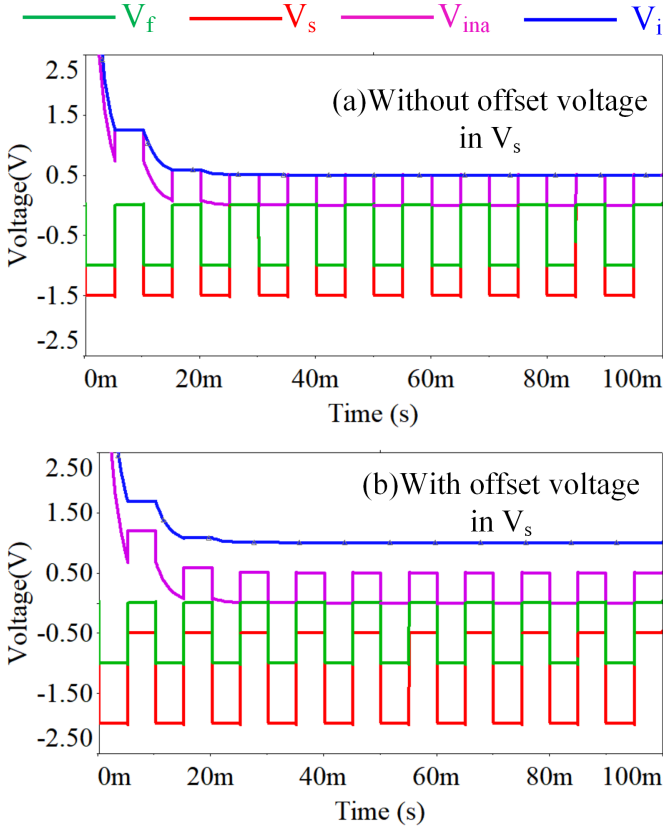


Fig. 2. Waveform at different nodes of the simulation of the proposed circuit without offset voltage and with offset voltage for $V_{cm} = 0$. (a) Without the offset-voltage, the output of the integrator is equal to the $I(R_{sen} - R_f)$ for $t_1 < \omega t < t_2$. (b) The amplitude of the voltage at the output of the integrator will change when the offset voltage in V_s is zero.

connected to the inverted V_{ina} , as shown in Fig. 1. The output voltage of the switch can be written as follows.

$$V_{sw}(t) = \begin{cases} V_{cm} & ; t_0 < \omega t < t_1 \\ I_{sen}(t)R_{sen} - I_f(t)R_f + V_{REF} & ; t_1 < \omega t < t_2 \end{cases} \quad (4)$$

The output voltage $V_{sw}(t)$ of switch S_1 is proportional to the incremental sensor resistance and is sampled by an Analog-to-Digital Converter (ADC), as shown in Fig. 1.

A. Baseline-Resistance and Offset-Voltage Compensation

- **Baseline Resistance:** The sensor's baseline resistance is usually large compared to the dynamic change in the resistance due to measurand. The current-excitation bridge provides a differential measurement to compensate for the BRD; however, it is difficult and time-consuming to manually tune the value of reference resistance R_f equal to the baseline resistance R_o . The automatic compensation of R_o using a digital potentiometer is possible; however, the finite resolution of the digital potentiometer and large tolerance value prevent the effective compensation of baseline resistance.

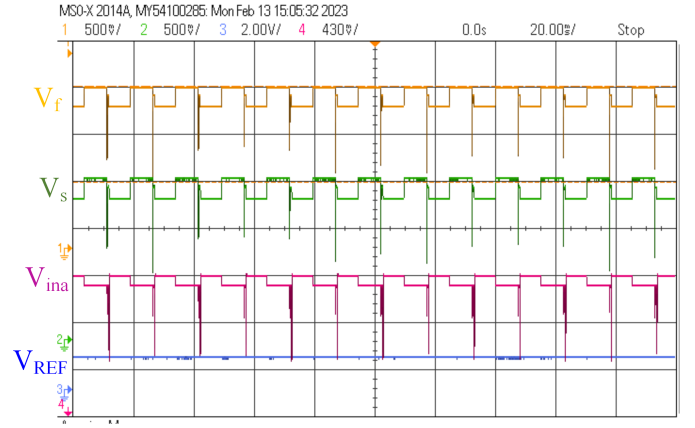


Fig. 3. Snapshot of the waveform recorded experimentally at the different nodes of the proposed circuit.

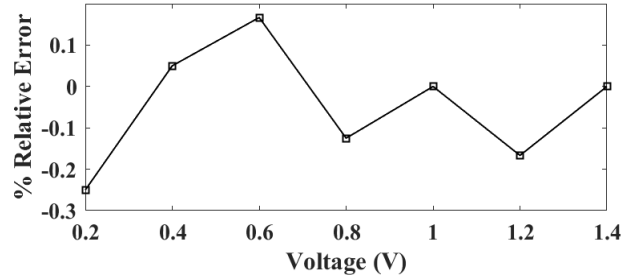


Fig. 4. Experimental results for the offset voltage compensation and the percentage relative error.

- **Offset Voltage:** The accuracy and resolution of the sensor systems are affected by the input-offset voltage and thermoelectric voltage. The effect of these voltages needs to be corrected for high-precision sensor systems.

Considering these, the output of the effective offset voltage as V_{of} at the output of the sensor branch, the expression for V_s can be rewritten as follows.

$$V_s = V_{cm} - I_{sen}(t)R_{sen} + V_{of} \quad ; t_1 < \omega t < t_2 \quad (5)$$

Further, considering R_m as the mismatch between the sensor resistance R_{sen} and reference resistance R_f and $I_{sen}(t) = I_f(t) = I(t)$, the expression (5) for the voltage V_{ina} at the output of instrumentation amplifier can be written as follows.

$$V_{ina} = I(t)R_m + V_{of} + V_{REF} \quad ; t_1 < \omega t < t_2 \quad (6)$$

The switch S_1 will demodulate the output of the instrumentation amplifier. A DC-servo loop is implemented to compensate for the effect of baseline resistance mismatch and offset voltage, as shown in Fig. 1. The feedback loop will force the output of the switch to settle at voltage V_{cm} , which is only possible when $V_{REF} = V_{cm} + IR_m + V_{of}$, where I is the amplitude of the current. The DC output voltage of the switch at this point is equal to V_{cm} .

TABLE I
COMPONENTS USED FOR THE PROTOTYPE

Component	Model
Current Sources (I_1 & I_2)	LM334
Operational Amplifiers (OA_1, OA_2, OA_3)	MCP6242
Instrumentation Amplifier (INA)	INA823
SPDT (S_1, S_2)	TS5A3160DCKT
Microcontroller with DAC and ADC	SAMD21

B. ΔR Measurement

Once the feedback loop compensates for the baseline resistance and the offset voltage, the equivalent voltage is generated by the digital-to-analog converter (DAC) and connected to the reference pin of the INA. At this instant, the output voltage of the switch S_1 is at V_{cm} , and ΔR of the resistive sensor is zero. After the calibration, the change in the resistance can be calculated by measuring the switch output voltage

$$V_{sw} = V_{cm} + I\Delta R \quad ; t_1 < \omega t < t_2 \quad (7)$$

III. EXPERIMENTAL SETUP AND RESULTS

The proposed circuit is implemented on a breadboard to test the performance. The components used to implement the system are tabulated in Table I. The circuit is powered with a supply voltage of 3.3 V. The common-mode voltage V_{cm} is kept at 1.65 V. The output waveform recorded experimentally is shown in Fig. 3.

Multiple experiments were conducted on the fabricated prototype to evaluate its performance.

A. Compensation of Offset-Voltage & BRD

First, the effect of offset-voltage and BRD is compensated using the proposed circuit. The experiment is conducted in two steps. First, the offset-voltage of different values is introduced using a DC supply in the sensor branch, and the variation in integrator output V_i is recorded. The BRD is considered constant in this case. Next, the offset-voltage is fixed, and the value of the BRD is varied. The integrator output is recorded. The equivalent voltage from the DAC is generated to compensate for the offset voltage and mismatch. The offset voltage is compensated from 0.2 Volts to 1.4 Volts from V_{cm} , as shown in Fig. 4. The mismatch in the sensor resistance is compensated from 10 $k\Omega$ to 100 $k\Omega$ with unity-gain of INA and from 1 $k\Omega$ to 10 $k\Omega$ for an INA with gain of 10. Fig. 5 shows the results for an INA having a gain of 10. The result shows that the proposed circuit is able to compensate the offset and mismatch with an accuracy of less than $\pm 1\%$.

B. ΔR Measurement

In this experiment, the incremental change in the sensor resistance ΔR is varied, and the output voltage of the switch (V_{sm}) is measured. The value of ΔR is varied from 2 $k\Omega$ to 14 $k\Omega$ in steps of 2 $k\Omega$, and the output voltage is recorded. The gain of INA is kept at 10. The recorded voltage for different ΔR values is shown in Fig. 6. The proposed system provides a resolution of around 10 Ω for a change in ΔR with an INA gain of 10 and $I = 10\mu A$.

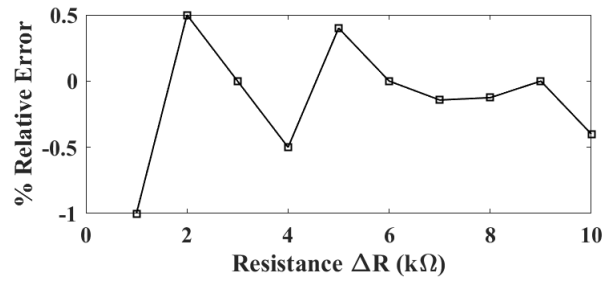


Fig. 5. Experimental results for the resistance mismatch compensation and the percentage relative error.

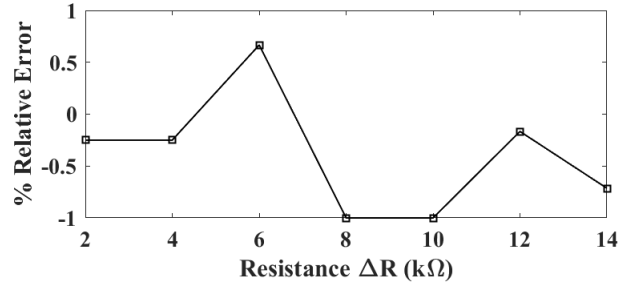


Fig. 6. Experimental results for the measurement of ΔR with the percentage relative error.

C. Performance Parameters and Discussion

The proposed system's performance parameters are measured, such as power consumption, resolution, and dynamic range. The power consumption of the proposed system is around 3 mW with a supply voltage of 3.3 Volts for analog blocks. The proposed system is able to compensate for the commutative offset voltage due to the input offset voltage, thermo-electric offset, and the resistance mismatch, as high as V_{cm} of the proposed circuit. The dynamic range for the ΔR for a supply current of 10 μA and a unity gain of INA is from 100 Ω to 160 $k\Omega$ with a resolution of around 80 Ω . The resolution of the proposed system can be increased by increasing the gain of the INA. However, the dynamic range will be reduced accordingly. The proposed circuit can be used standalone or with the digital potentiometer for fine compensation of the BRD and offset voltage for a wide range of high-resolution and high-accuracy sensing applications.

IV. CONCLUSION

An offset-voltage and resistance mismatch compensation technique for resistive sensors is proposed in this paper. A pulse current excitation signal was used to modulate the sensor signal. The feedback loop compensates for the mismatch between the sensor and reference signal and the dc-offset at the output of the instrumentation amplifier. If not canceled, these mismatches and offset voltage affect the accuracy and measurement range of the resistive sensor system. The proposed system is experimentally validated for an offset voltage as high as ± 1.4 V from the common-mode voltage V_{cm} for a supply voltage of 3.3 V. In addition, the system is tested

with a resistance mismatch as high as $100\text{ k}\Omega$. The developed system is able to compensate for offset and mismatch with an error of less than $\pm 1\%$.

REFERENCES

- [1] R. Zamparetti and K. Makinwa, "A 2.5- μw beyond-the-rails current sensor with a tunable voltage reference and $\pm 0.6^\circ\text{C}$," *IEEE Solid-State Circuits Letters*, vol. 5, pp. 264–267, 2022.
- [2] S. Pan, J. A. Angevare, and K. A. A. Makinwa, "5.4 a hybrid thermal-diffusivity/resistor-based temperature sensor with a self-calibrated inaccuracy of $\pm 0.25^\circ\text{C}$ from -55°C to 125°C ," in *2021 IEEE International Solid-State Circuits Conference (ISSCC)*, vol. 64, 2021, pp. 78–80.
- [3] R. A. Romeo, C. Lauretti, C. Gentile, E. Guglielmelli, and L. Zollo, "Method for automatic slippage detection with tactile sensors embedded in prosthetic hands," *IEEE Transactions on Medical Robotics and Bionics*, vol. 3, no. 2, pp. 485–497, 2021.
- [4] B. Yao, Y. Dai, G. Xia, Z. Zhang, and J. Zhang, "High-sensitivity and wide-range resistance measurement based on self-balancing wheatstone bridge and gated recurrent neural network," *IEEE Transactions on Industrial Electronics*, vol. 70, no. 5, pp. 5326–5335, 2023.
- [5] L. Somappa, S. Malik, M. Ahmad, K. M. Ehsan, A. M. Shaikh, D. Berwal, S. Sonkusale, and M. S. Baghini, "Design and development of a robotic hand with embedded sensors using 3d printing technology," *Transactions of the Indian National Academy of Engineering*, 2021.
- [6] N. Samaddar, M. I. Wani, V. Maharshi, S. Sonkusale, and S. Malik, "A resistance change detection circuitry for thread based resistive sensors," in *2023 IEEE Applied Sensing Conference (APSCON)*, 2023, pp. 1–3.
- [7] J. C. Yang, J. Mun, S. Y. Kwon, S. Park, Z. Bao, and S. Park, "Electronic skin: Recent progress and future prospects for skin-attachable devices for health monitoring, robotics, and prosthetics," *Advanced Materials*, vol. 31, no. 48, p. 1904765, 2019. [Online]. Available: <https://onlinelibrary.wiley.com/doi/abs/10.1002/adma.201904765>
- [8] A. D. Marcellis and G. Ferri, *Analog Circuit and System for Voltage-mode and Current-mode Sensor Interfacing Application*,. New Delhi, India: Springer, 2011.
- [9] J. Fraden, *Handbook of Modern Sensors: Physics, Designs, and Applications*. New Delhi, India: Springer, 2010.
- [10] W. G. Jung, *OP AMP applications handbook*. Newnes, 2005.
- [11] D. PDF, "Linearization of wheatstone-bridge." [Online]. Available: <https://www.analog.com/en/technical-articles/how-to-linearize-wheatstonebridge-circuit-for-better-performance.html>
- [12] K. Hoffmann, *Applying the Wheatstone Bridge Circuit*. HBM, 1974.
- [13] A. De Marcellis, G. Ferri, and P. Mantenuto, "Analog wheatstone bridge-based automatic interface for grounded and floating wide-range resistive sensors," *Sensors and Actuators B: Chemical*, vol. 187, pp. 371–378, 2013, selected Papers from the 14th International Meeting on Chemical Sensors. [Online]. Available: <https://www.sciencedirect.com/science/article/pii/S0925400512013536>
- [14] K. Kishore, S. Malik, M. S. Baghini, and S. A. Akbar, "A dual-differential subtractor-based auto-nulling signal conditioning circuit for wide-range resistive sensors," *IEEE Sensors Journal*, vol. 20, no. 6, pp. 3047–3056, 2020.
- [15] S. Kumar, S. S. Khan, R. Patil, M. Ahmad, L. Somappa, and S. Malik, "Development and validation of offset current compensation technique for optical sensors," in *2023 IEEE Applied Sensing Conference (APSCON)*, 2023, pp. 1–3.
- [16] S. Malik, M. Ahmad, L. Somappa, T. Islam, and M. S. Baghini, "An-z2v: Autonulling-based multimode signal conditioning circuit for r-c sensors," *IEEE Transactions on Instrumentation and Measurement*, vol. 69, no. 11, pp. 8763–8772, 2020.
- [17] S. Malik, K. Kishore, L. Somappa, S. Lashkare, T. Islam, S. A. Akbar, and M. Shojaei Baghini, "A dual-slope-based capacitance-to-time signal conditioning circuit for leaky capacitive sensors," *IEEE Transactions on Instrumentation and Measurement*, vol. 70, pp. 1–8, 2021.
- [18] S. Malik, L. Somappa, M. Ahmad, and M. S. Baghini, "An accurate auto-tunable quadrature-phase generator circuit for robust sensing applications," in *2020 IEEE 17th India Council International Conference (INDICON)*, 2020, pp. 1–5.
- [19] A. Mohamed, M. Wagner, H. Heidari, and J. Anders, "A frontend for magnetoresistive sensors with a 2.2-pa/hz low-noise current source," *IEEE Solid-State Circuits Letters*, vol. 5, pp. 17–20, 2022.
- [20] A. Mohamed, H. Heidari, and J. Anders, "A readout circuit for tunnel magnetoresistive sensors employing an ultra-low-noise current source," in *ESSCIRC 2021 - IEEE 47th European Solid State Circuits Conference (ESSCIRC)*, 2021, pp. 331–334.
- [21] N. A. Gilda, S. Nag, S. Patil, M. S. Baghini, D. K. Sharma, and V. R. Rao, "Current excitation method for δR measurement in piezo-resistive sensors with a 0.3-ppm resolution," *IEEE Transactions on Instrumentation and Measurement*, vol. 61, no. 3, pp. 767–774, 2012.
- [22] V. S. Palaparthi, S. N. Doddapujar, G. Gupta, P. Das, S. A. Chandorkar, S. Mukherji, M. S. Baghini, and V. R. Rao, "E-nose: Multichannel analog signal conditioning circuit with pattern recognition for explosive sensing," *IEEE Sensors Journal*, vol. 20, no. 3, 2020.
- [23] M. Ahmad, S. Malik, H. Patel, and M. S. Baghini, "A portable low-voltage low-power ppm-level resistive sensor measurement system," *IEEE Sensors Journal*, vol. 22, no. 3, pp. 2338–2346, 2022.